Eigenstate thermalization hypothesis and quantum Jarzynski relation for pure initial states

F. Jin,[1,*] R. Steinigeweg,[2,†] H. De Raedt,[3] K. Michielsen,[1,4] M. Campisi,[5,‡] and J. Gemmer[2,§]

[1]*Institute for Advanced Simulation, Jülich Supercomputing Centre, Forschungszentrum Jülich, D-52425 Jülich, Germany*
[2]*Department of Physics, University of Osnabrück, D-49069 Osnabrück, Germany*
[3]*Zernike Institute for Advanced Materials, University of Groningen, NL-9747AG Groningen, The Netherlands*
[4]*RWTH Aachen University, D-52056 Aachen, Germany*
[5]*NEST, Scuola Normale Superiore & Istituto Nanoscienze-CNR, I-56126 Pisa, Italy*

Since the first suggestion of the Jarzynski equality many derivations of this equality have been presented in both the classical and the quantum context. While the approaches and settings differ greatly from one another, they all appear to rely on the condition that the initial state is a thermal Gibbs state. Here, we present an investigation of work distributions in driven isolated quantum systems, starting from pure states that are close to energy eigenstates of the initial Hamiltonian. We find that, for the nonintegrable quantum ladder studied, the Jarzynski equality is fulfilled to a good accuracy.

I. INTRODUCTION

The last decades have witnessed renewed interest in the old question whether and how closed finite quantum systems approach thermal equilibrium. Equilibration and thermalization have been theoretically discussed for both fairly abstract [1–6] and more specific systems of condensed-matter type [7–10]. Key concepts in this discussion are typicality (or concentration of measure) and the eigenstate thermalization hypothesis (ETH). With the advent of experiments on ultracold atoms, some of the theoretical results have even become testable. As of today, the mere existence of some sort of equilibrium in closed quantum systems has been the most widely addressed question. However, lately the dynamical approach to equilibrium has been intensely investigated [11,12]. Here, crucial questions are the relaxation times but also the degree of agreement of quantum dynamics with standard statistical relaxation descriptions by master or Fokker-Planck equations, stochastic processes, etc. [13–15]. The crucial feature that discriminates these types of analysis from standard open-systems concepts, like quantum master equations, is the fact that the statistical dynamics emerge from the systems themselves, i.e., are not induced by any bath.

Also fluctuation theorems have been and continue to be a central topic in the field of statistical mechanics [16]. The Jarzynski relation (JR), making general statements on work that has to be invested to drive processes also and especially far from equilibrium, is a prime example of such a fluctuation theorem. Many derivations of the JR from various starting grounds have been presented. These include classical Hamiltonian dynamics, stochastic dynamics such as Langevin or master equations, and quantum mechanical starting points [16–20]. However, all these derivations assume that the system, which is acted on with some kind of "force," is strictly in a Gibbsian equilibrium state before the process starts. This starting point

differs from the progress in the field of thermalization: There, the general features of thermodynamical relaxation are found to emerge entirely from the system itself, without the necessity of evoking external baths or specifying initial states in detail. Clearly, the preparation of a strictly Gibbsian initial state requires coupling to a bath prior to starting the process.

In this paper, we study the question whether or not the JR is valid with a system starting in a state other than a Gibbs state. Since counterexamples can be constructed, any affirmative answer cannot hold for any quantum system and for any process protocol. In fact, previous works [21–24] have shown that, when the initial state is microcanonical, the JR does not follow, but a related entropy-from-work relation emerges instead. The question remains, however, whether and under what conditions the JR holds approximately for noncanonical initial states. Thus, the emphasis in the search for the origins of the JR's validity is shifted from specifying the initial state to specifying the nature of the system.

II. JARZYNSKI RELATION AND EIGENSTATE THERMALIZATION HYPOTHESIS

To further clarify this, consider the standard setup of the quantum JR for closed systems. It is based on a two-measurement scheme: If the system is at energy E_{ini} before the process, then there is a conditional probability,

$$T = T(E_{\text{fin}}|E_{\text{ini}},\lambda(t)) \qquad (1)$$

[with $\lambda(t)$ being the protocol], of finding the system at E_{fin} after the process [25]. Let $W = E_{\text{fin}} - E_{\text{ini}}$ be the work associated with this transition. The average of the exponentiated work $\langle e^{-\beta W} \rangle$ can now be written as

$$\langle e^{-\beta W} \rangle = \sum_{E_{\text{fin}}, E_{\text{ini}}} T \, e^{-\beta(E_{\text{fin}} - E_{\text{ini}})} \, P_{\text{ini}}(E_{\text{ini}}). \qquad (2)$$

Obviously, $\langle e^{-\beta W} \rangle$ depends on $P_{\text{ini}}(E_{\text{ini}})$. It is well known that the JR

$$\langle e^{-\beta W} \rangle = e^{-\beta \Delta F} \qquad (3)$$

(with ΔF being the change in the free energy F) always holds for initial Gibbs states $P_{\text{ini}}(E_{\text{ini}}) \propto e^{-\beta E_{\text{ini}}}$, regardless of the

system and the protocol. Much less is known about other initial states, e.g., initial energy eigenstates $P_{\text{ini}}(E_{\text{ini}}) \approx \delta_{E_{\text{ini}}, E_n}$, with E_n being the energy of an eigenstate. We study these states here.

It is very important to note that this question can be recast as a question about the validity of the ETH in a specific sense: As shown in [21], the average exponentiated work can be written as the expectation value

$$\langle e^{-\beta W} \rangle = \langle e^{-\beta H_{\text{fin}}^H} e^{\beta H_{\text{ini}}} \rangle_{\text{diag}}, \qquad (4)$$

where $H_{\text{fin/ini}}$ are the final and initial Hamiltonians (with the index H indicating the Heisenberg picture) and $\langle \cdots \rangle_{\text{diag}}$ denotes the average over the diagonal part of the initial density matrix with regard to the eigenbasis of H_{ini} [21]. Let $\langle \cdots \rangle_{\text{can/mic}}$ denote averages over canonical and microcanonical states, which are both diagonal in the above sense. While the standard JR $\langle e^{-\beta W} \rangle = \langle e^{-\beta H_{\text{fin}}^H} e^{-\beta H_{\text{ini}}} \rangle_{\text{can}} = e^{-\beta \Delta F}$ always holds, our questions can be reformulated as

$$\langle e^{-\beta H_{\text{fin}}^H} e^{\beta H_{\text{ini}}} \rangle_{\text{mic}} \overset{?}{=} \langle e^{-\beta H_{\text{fin}}^H} e^{\beta H_{\text{ini}}} \rangle_{\text{can}}, \qquad (5)$$

where the left-hand side (l.h.s.) is the average for a microcanonical state living inside an arbitrarily narrow energy shell which is located at the mean energy of the respective Gibbsian state at inverse temperature β. The validity of Eq. (5) is claimed by the ETH (even though the operator in the average is non-Hermitian). Since each protocol yields a different H_{fin}^H, the JR's validity for microcanonical states is equivalent to the ETH's validity for a set of different operators. So far, however, no general principle guarantees the applicability of the ETH, except for large quantum systems with a direct classical counterpart [26] or systems involving random matrices [27]. While the ETH is expected to hold for nonintegrable systems and few-body observables, $e^{-\beta H_{\text{fin}}^H} e^{\beta H_{\text{ini}}}$ is not such an operator. Thus, investigating the JR's validity for microcanonical states is a highly nontrivial endeavor.

In this paper, we use numerical methods to prepare an energetically firmly concentrated initial state and to propagate it according to the Schrödinger equation for a complex spin system with a strongly time-dependent Hamiltonian. Since the initial state is sharp in energy, the eventual energy-probability distribution is interpreted as a work-probability distribution and thus checked for agreement with the JR, including a careful finite-size scaling. As there is no thermal initial state, we use for the inverse temperature β in the JR the standard definition $\beta = dS/dE$ and resort to the microcanonical entropy $S = \ln n(E)$, where $n(E)$ is the density of energy eigenstates (DOS). Thus,

$$\beta = \frac{d}{dE} \ln n(E). \qquad (6)$$

Obviously, β depends on the spectrum. Since β also depends on E, we evaluate β at the initial energy E_{ini}.

III. SPIN MODEL AND TIME-DEPENDENT MAGNETIC FIELD

We consider a specific model with specific parameters. This model is a prime example for the emergence of thermodynamical behavior in closed, small quantum systems. In particular, the quantum dynamics of certain observables is in remarkably
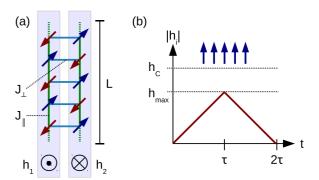

FIG. 1. Sketch of (a) the Heisenberg $S = 1/2$ ladder studied and (b) the time-dependent magnetic field applied. This magnetic field induces magnetization in the two legs.

good accord with an irreversible Fokker-Plank equation for the undriven system and with a Markovian stochastic process in a more detailed sense [13].

As shown in Fig. 1, we study an anisotropic spin-1/2 Heisenberg ladder with the rung coupling being significantly weaker than the leg coupling. Specifically, the Hamiltonian $H = J_\parallel H_\parallel + J_\perp H_\perp$ consists of a leg part $H_\parallel$ and a rung part $H_\perp$,

$$H_\parallel = \sum_{i=1}^{L-1} \sum_{k=1}^{2} S_{i,k}^x S_{i+1,k}^x + S_{i,k}^y S_{i+1,k}^y + \Delta S_{i,k}^z S_{i+1,k}^z,$$
$$\qquad (7)$$
$$H_\perp = \sum_{i=1}^{L} S_{i,1}^x S_{i,2}^x + S_{i,1}^y S_{i,2}^y + \Delta S_{i,1}^z S_{i,2}^z,$$

where $S_{i,k}^{x,y,z}$ are spin-1/2 operators at site (i,k). $J_{\parallel,\perp} > 0$ are antiferromagnetic exchange coupling constants with $J_\perp = 0.2 \, J_\parallel$, $\Delta = 0.6$ is the exchange anisotropy in the z direction, and L is the number of sites in each leg. We set $J_\parallel = 1$ throughout this work.

A magnetic field $h(t)$ is turned on once the time evolution starts. The field is uniform along each individual leg, pointing in the positive z direction on one leg and in the negative z direction on the other. This field is linearly ramped up in time from 0 to h_{max} for a certain time τ and then linearly ramped down for the same time with the same slope. Thus, the field starts at 0 and ends at 0, i.e., the initial and final Hamiltonians are identical. More precisely, we model the field by

$$h(t) = -h_{\text{max}} f(t) \left(S_1^z - S_2^z \right), \qquad (8)$$

with the total leg magnetization

$$S_k^z = \sum_{i=1}^{L} S_{i,k}^z \qquad (9)$$

and the time dependence

$$f(t) = \begin{cases} t/\tau, & 0 < t \leqslant \tau, \\ 2 - t/\tau, & \tau < t \leqslant 2\tau. \end{cases} \qquad (10)$$

The full Hamiltonian is $H_{\text{tot}}(t) = H + h(t)$. Note that this protocol renders the initial and final Hamiltonians identical. This avoids the difficulties of defining free energies for non-Gibbsian states [cf. Eq. (15)]. (For a more elaborate approach to this issue see Ref. [38]). We choose the field
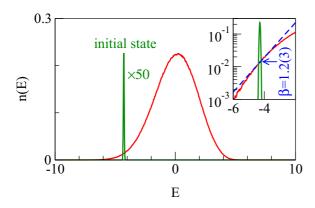
FIG. 2. DOS $n(E)$ for the Heisenberg $S = 1/2$ ladder in Eq. (7) with $J_\perp = 0.2 J_\parallel$, $\Delta = 0.6$, and $L = 11$. Due to the method used to obtain the numerical data, the energy resolution 0.007(6) is high but finite. The initial state prepared is also indicated. Inset: Same as the figure but in a semilog plot and with the inverse temperature $\beta = 1.2(3)$ indicated.

strength $h_{max} = 0.5$ for all simulations and vary the sweep time τ.

To specify a quantity that plays the role of temperature, we must have information on the DOS of H. Since the numerical diagonalization of H is unfeasible for the system sizes we are interested in, we resort to the numerical method described in [28]. This method is incapable of resolving individual energy eigenvalues but captures rather accurately the coarser features of the DOS; see Appendix A 3 for details. The result for our Hamiltonian is displayed in Fig. 2.

We choose the initial energy E_{ini} to locate the process at a nonpeculiar temperature regime, i.e., neither extremely high nor very low (nor negative) temperatures but an intermediate regime on the natural scale of the model, $\beta \sim 1/J_\parallel$. To this end, we prepare an initial state that is energetically firmly concentrated at $E_{ini} = -4.2(8)$ for $L = 11$. Using the definition $\beta = d/dE \ln n(E)$ yields $\beta = 1.2(3)$. It is worth pointing out that, in this energy regime, β does not vary much on an interval of ca. $2J_\parallel$, which is about the overall scale of the work required for our process.

IV. PREPARATION AND CHARACTERIZATION OF THE INITIAL STATE

We prepare a state of the form

$$|\Psi(a, E_{ini})\rangle = \frac{e^{-a(H - E_{ini})^2/4} |\Phi\rangle}{\langle \Phi | e^{-a(H - E_{ini})^2/2} |\Phi\rangle}, \quad (11)$$

where $|\Phi\rangle$ is a random state drawn according to the Haar measure on the total Hilbert space. Obviously, $|\Psi(a, E_{ini})\rangle$ is always centered at the energy E_{ini} with a variance $\propto 1/a$. (Note that the Gaussian form is chosen only for technical reasons and thus unrelated to, e.g., the Gaussian expansion coefficients as discussed in Ref. [26].) Clearly, since $|\Phi\rangle$ is random, any quantity Q calculated from $|\Psi(a, E_{ini})\rangle$ is random. However, as shown (and applied [10,29,30]) in the context of typicality, the average

$$\bar{Q} = \overline{\langle \Psi(a, E_{ini}) | Q | \Psi(a, E_{ini}) \rangle} \quad (12)$$

equals a mixed-state expectation value, i.e.,

$$\bar{Q} = \mathrm{Tr}\{\rho Q\}, \quad \rho = \frac{e^{-a(H - E_{ini})^2/2}}{\mathrm{Tr}\{e^{-a(H - E_{ini})^2/2}\}}. \quad (13)$$

Moreover, the statistical error

$$\epsilon = \sqrt{\overline{(Q^2)} - (\bar{Q})^2} \propto 1/\sqrt{\mathrm{Tr}\{e^{-a(H - E_{ini})^2/2}\}} \quad (14)$$

is very small if the Hilbert space is large (but a is not too large). Investing a reasonable computational effort, we are able to reach $a = 1000$. In this regime, ϵ is negligibly small; see Appendix B 3.

Using the same method as for calculating the DOS, we illustrate the probability distribution of a state $|\Psi(a, E_{ini})\rangle$ in Fig. 2. Clearly, this distribution is firmly concentrated at $E_{ini} = -4.2(8)$.

V. PROCESS, FINAL ENERGY DISTRIBUTION, AND JARZYNSKI RELATION

Now, we perform the simulation of the actual process. To this end, we propagate $|\Psi(a, E_{ini})\rangle$ in time according to the Schrödinger equation using the time-dependent Hamiltonian $H_{tot}(t) = H + h(t)$ (see Appendix A 1 for details). We do so for different sweep rates $\gamma = 1/(2\tau)$, ranging from slow driving, $\gamma_0 = 2.6 \times 10^{-4}$, to fast driving, $\gamma = 150\gamma_0$. This yields a set of final energy-probability distributions $P_{fin}(E, \gamma)$ (see Fig. 3). Clearly, these distributions shift towards higher
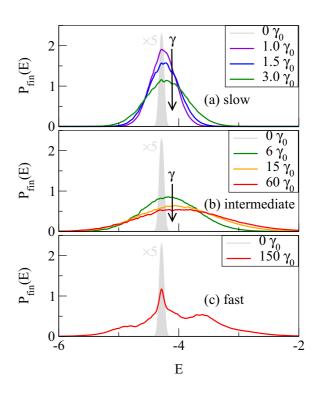

FIG. 3. Probability distribution $P_{fin}(E)$ of the final state for (a) weak, (b) intermediate, and (c) fast driving. (The remaining parameters are identical to those for Fig. 2.) Due to the initial state being almost an energy eigenstate, this distribution almost coincides with the probability distribution of work.

energies and broaden with increasing γ. Furthermore, they develop distinctly non-Gaussian features.

Let us compare this result against the JR, which here, since the initial and the final Hamiltonians are the same, reads

$$\langle e^{-\beta W} \rangle = \int P_W(W) e^{-\beta W} dW = 1. \tag{15}$$

If the initial state was a true energy eigenstate at energy $E = E_{\text{ini}}$, then it would be justified to infer the actual probability distribution of work P_W from P_{fin} as $P_W(W) = P_{\text{fin}}(W + E_{\text{ini}})$. In this case the latter expression could be used to check Eq. (15) directly. Given the "narrowness" of P_{ini}, it seems plausible that the actual work-probability distribution $P_W(W)$ must be close to $P_{\text{fin}}(W + E_{\text{ini}})$. However, since P_{ini} is not precisely a δ distribution, one cannot, strictly speaking, conclude from P_{fin} onto P_W.

To nonetheless do so, we employ a very natural assumption: It is plausible that the P_W resulting from an initial δ peak should not vary significantly with a slight change in the position of this peak. Under this assumption, we can take into account the finite, yet very narrow width of our initial state by a convolution of distributions (see Appendix B 2). Using simple math, the l.h.s. of Eq. (15) can be cast in the form

$$\frac{\int P_{\text{fin}}(E_{\text{fin}}) e^{-\beta E_{\text{fin}}} dE_{\text{fin}}}{\int P_{\text{ini}}(E_{\text{ini}}) e^{-\beta E_{\text{ini}}} dE_{\text{ini}}} = \int P_W(W) e^{-\beta W} dW. \tag{16}$$

Thus, the l.h.s. of Eq. (16) yields $\langle e^{-\beta W} \rangle$ based on P_{fin}, P_{ini} for different sweep rates γ. The closeness of the outcome to 1 indicates how well the JR is fulfilled. As shown in Fig. 4, for very slow processes the l.h.s. of Eq. (16) is practically 1, while
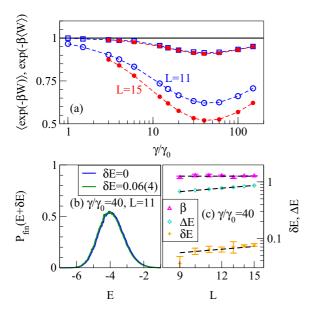

FIG. 4. (a) Averages $\langle e^{-\beta W} \rangle$ (squares) and $e^{-\beta \langle W \rangle}$ (circles) as a function of the process rate γ for two L values, $L = 11$ and 15 sites, and initial energies corresponding to the inverse temperature $\beta \approx 1.2$. (b) Final distribution $P_{\text{fin}}(E)$ and fictitious distribution $P_{\text{fin}}(E + \delta E)$ for $L = 11$ and the rate $\gamma = 40\gamma_0$, where the deviation of $\langle e^{-\beta W} \rangle$ from 1 is largest in (a). (c) Finite-size scaling of β, ΔE, and δE for the γ in (b). All error bars indicated in (b) correspond to errors resulting when determining β by fitting the DOS locally.

there is a difference of ca. 0.1 for faster processes. Comparing this difference to the deviation of $e^{-\beta \langle W \rangle}$ from 1 points to the approximate validity rather than a strong violation of the JR.

We note that in the limits of $\gamma \to 0$ and $\gamma \to \infty$ the JR is trivially fulfilled: While for $\gamma \to 0$ the system has sufficient time to follow adiabatically, for $\gamma \to \infty$ the system has no time to react.

VI. DISCUSSION

A. Energy shift

To examine this further, we use the following scheme: For every actual $P_{\text{fin}}(E_{\text{fin}})$ there is a fictitious probability distribution $\mathcal{P}(E_{\text{fin}}) := P_{\text{fin}}(E_{\text{fin}} + \delta E)$, which is identical in shape but shifted in energy by δE and fulfills the JR exactly; i.e., Eq. (16) with $P_{\text{fin}} \to \mathcal{P}$ is identical to 1. We use this equation to identify δE and get $\delta E = 0.06(4)$ for $L = 11$ and for $\gamma = 40\gamma_0$, where the deviation of the l.h.s. of Eq. (16) from 1 is the largest. In Fig. 4(b) we display $\mathcal{P}(E_{\text{fin}})$ together with $P_{\text{fin}}(E_{\text{fin}})$. Clearly, the difference is hardly visible, as δE is much smaller than the standard deviation $\Delta E = 0.7(4)$ of either distribution. Thus, while the JR is clearly violated, the smallness of δE indicates that this violation is remarkably small.

It should be stressed that the JR exponentially amplifies errors in the negative tail of the distribution [31], i.e., a tiny lack of statistics in this tail can in principle result in a large deviation from the JR (the observed non-negativity of δE probably reflects this occurrence). This implies that one needs roughly an exponential number of samples to get a good estimate of the average exponentiated work [32] even for initial canonical states. In this sense the observed deviation from the JR of at most 10%, obtained from a single wave function, is indeed small and a central result of this paper.

For all other sweep rates, δE turns out to be even smaller, thus rendering the actual work-probability distribution even closer to the fictitious one. Note that the fictitious probability distribution $\mathcal{P}(E_{\text{fin}})$ introduced is certainly not the only choice possible. However, it allows for a very natural interpretation.

B. Finite-size scaling

Finally, we perform a finite-size scaling for $L = 9, \ldots, 15$ and $E_{\text{ini}} = -0.42(L - 1)$, yielding $\beta \approx 1.2$ within the attainable precision. Focusing on $\gamma = 40\gamma_0$, with the largest violation of the JR, we depict the scaling $\Delta E(L)$ and $\delta E(L)$ in Fig. 4(c). While $\Delta E(L)$ follows a "trivial" upscaling $\Delta E(L) \propto \sqrt{L}$ (see Appendix B 5), giving a precise statement of $\delta E(L)$ remains challenging. Given the error bars shown, resulting from errors when determining β by fitting, a very reasonable guess is $\delta E(L) \propto \sqrt{L}$, indicated in Fig. 4(c). Then, $\delta E(L)/\Delta E(L) = \text{const.}$ and we can expect that the JR remains valid to a very good approximation for $L \to \infty$.

VII. CONCLUSIONS

In summary, we have studied the validity of the JR for noncanonical initial states that are pure states close to energy eigenstates. To this end, we have performed large-scale numerics first to prepare typical states of this kind and then

to propagate these states under a time-dependent protocol in a complex quantum system of condensed-matter type. While we have found violations of the JR in our nonequilibrium scenario, we have demonstrated that these violations are remarkably small and point to the approximative validity of the JR in a moderately sized system already. Furthermore, our systematic finite-size analysis has not shown indications that this result changes in the thermodynamic limit of very large systems.

While this result cannot be simply explained by the equivalence of ensembles, it indicates the validity of the ETH for a nontrivial operator being the "operator of exponentiated work." This validity is surprising due to the structure of this operator but also since the ETH is commonly associated with equilibrium properties, while the JR addresses nonequilibrium processes. Promising directions of future research include the generality of our findings for a wider class of systems and protocols, the necessity of the two-measurement scheme, and the dependence of the work distribution as such on the type of initial condition realized.

APPENDIX A: NUMERICAL METHOD

1. Time-dependent Schrödinger equation (TDSE)

The full Hamiltonian of the spin-$1/2$ ladder system reads $\mathcal{H}(t) = H + h(t)$, where H and $h(t)$ are defined by Eqs. (7) and (8). Here, to shorten the notation, we write $\mathcal{H}(t)$ instead of $H_{\text{tot}}(t)$. The time evolution of the system is governed by the TDSE (in units of $\hbar = 1$),

$$i \frac{\partial}{\partial t} |\Psi(t)\rangle = \mathcal{H}(t)|\Psi(t)\rangle, \tag{A1}$$

where $|\Psi(t)\rangle$ is the wave function of the system. The solution of the TDSE can be written as

$$|\Psi(t + \delta t)\rangle = U(t + \delta t, t)|\Psi(t)\rangle,$$
$$U(t + \delta t, t) = \exp_+\left(-i \int_t^{t+\delta t} \mathcal{H}(u)\, du\right), \tag{A2}$$

where δt is the time step. For small δt, the Hamiltonian is considered to be fixed in the time interval $[t, t + \delta t]$ and then the time-evolution operator may be approximated by

$$U(\delta t) = U(t + \delta t, t) = \exp(-i\mathcal{H}(t + \delta t/2)\delta t). \tag{A3}$$

We solve the TDSE using a second-order product-formula algorithm [34,35]. The basic idea of the algorithm is to use a second-order approximation of the time-evolution operator $U(\delta t)$, given by

$$\widetilde{U}_2(\delta t) = e^{-i\delta t \mathcal{H}_k/2} \dots e^{-i\delta t \mathcal{H}_1/2}$$
$$\times e^{-i\delta t \mathcal{H}_1/2} \dots e^{-i\delta t \mathcal{H}_k/2}, \tag{A4}$$

where $\mathcal{H} = \mathcal{H}_1 + \cdots + \mathcal{H}_k$. The approximation is bounded by

$$||U(\delta t) - \widetilde{U}_2(\delta t)|| \ll c_2\, \delta t^3, \tag{A5}$$

where c_2 is a positive constant.

In practice, we use the *XYZ* decomposition, i.e., $\mathcal{H} = \mathcal{H}_x + \mathcal{H}_y + \mathcal{H}_z$, where x, y, and z denote the components of the spin operators. The computational basis states are eigenstates of the S^z operators. In this representation $e^{-i\delta t \mathcal{H}_z}$ is diagonal by construction and changes only the state by altering the phase of each of the basis vectors. By a simple rotation of the basis, the operator $e^{-i\delta t \mathcal{H}_x}$ (or $e^{-i\delta t \mathcal{H}_y}$) becomes diagonal and affects only the phases of the individual rotated basis vectors. The inverse rotation transforms the rotated basis vectors back to the computational basis.

2. Initial state

The initial state is obtained by a Gaussian projection of a random state drawn at random according to the Haar measure on the total Hilbert space of the system,

$$|\Psi(a, E)\rangle = \frac{e^{-a(H-E)^2/4}|\Phi\rangle}{\langle\Phi| e^{-a(H-E)^2/2}|\Phi\rangle} \tag{A6}$$

[cf. Eq. (11)], where $1/a$ characterizes the variance of the Gaussian projection and H is the Hamiltonian at $t = 0$. This calculation is performed by employing the Chebyshev-polynomial representation of a Gaussian function, properly generalized to matrix-valued functions [36,37], and yields numerical results which are accurate to about 14 digits.

In general, a function $f(x)$ whose values are in the range $[-1, 1]$ can be expressed as

$$f(x) = \frac{1}{2}c_0 T_0(x) + \sum_{k=1}^{\infty} c_k T_k(x), \tag{A7}$$

where $T_k(x) = \cos(k \arccos x)$ are Chebyshev polynomials and the coefficients c_k are given by

$$c_k = \frac{2}{\pi} \int_{-1}^{1} \frac{dx}{\sqrt{1 - x^2}}\, f(x)\, T_k(x). \tag{A8}$$

Let $x = \cos\theta$; then $T_k(x) = \cos(k\theta)$ and

$$c_k = \frac{2}{\pi} \int_0^{\pi} f(\cos\theta) \cos(k\theta)\, d\theta$$
$$= \text{Re}\left[\frac{2}{N} \sum_{n=0}^{N-1} f\left(\cos\frac{2\pi n}{N}\right) e^{2\pi i n k/N} \right], \tag{A9}$$

which can be calculated by the fast Fourier transform.

For the operator $f(H) = e^{-a(H-E)^2/4}$, we normalize H such that $\widetilde{H} = H/||H||$ has eigenvalues in the range $[-1, 1]$ and set $\widetilde{a} = a||H||$ and $\widetilde{E} = E/||H||$. Then

$$f(\widetilde{H}) = e^{-\widetilde{a}(\widetilde{H}-\widetilde{E})^2/4} = \sum_{k=0}^{\infty} c_k T_k(\widetilde{H}), \tag{A10}$$

where c_k are the Chebyshev-expansion coefficients calculated from Eq. (A9) and the Chebyshev polynomial $T_k(\widetilde{H})$ can be obtained by the recursion relation

$$T_{k+1}(\widetilde{H}) - 2\widetilde{H} T_k(\widetilde{H}) + T_{k-1}(\widetilde{H}) = 0, \tag{A11}$$

with $T_0(\widetilde{H}) = 1$ and $T_1(\widetilde{H}) = \widetilde{H}$.

In practice, the coefficients c_k become numerically 0 for a certain $k \geqslant K$. Hence, the sum of K terms in Eq. (A10) is a numerically exact representation of the Gaussian projector. Recall that the Chebyshev algorithm can be efficiently applied to solve the TDSE only if the total Hamiltonian is time independent [37], which is the case for the Gaussian projector.

3. Density of states

The DOS of a quantum system may, in terms of the time evolution, be defined as

$$n(E) = \sum_n \delta(E - E_n)$$

$$= \frac{1}{2\pi} \int_{-\infty}^{+\infty} e^{itE} \, \mathrm{Tr}\{e^{-itH}\} \, \mathrm{d}t, \qquad \text{(A12)}$$

where H is the Hamiltonian of the system at $t = 0$ and n runs over all eigenvalues E_n of H. The trace in the integral can be estimated from the expectation value with respect to a random vector, e.g., by exploiting quantum typicality [10,28]. Thus, we have

$$\frac{\mathrm{Tr}\{e^{-itH}\}}{D} \approx \langle \Phi(0)|e^{-itH}|\Phi(0)\rangle = \langle \Phi(0)|\Phi(t)\rangle, \quad \text{(A13)}$$

where D is the dimension of the Hilbert space and $|\Phi(0)\rangle$ is a pure state drawn at random according to the unitary invariant measure (Haar measure) and the error scales with $1/\sqrt{D}$. $|\Phi(t)\rangle = e^{-itH}|\Phi(0)\rangle$ can be efficiently computed by the second-order product-formula algorithm. Therefore, the DOS can be conveniently calculated as

$$n(E) \approx C \int_{-\Theta}^{+\Theta} e^{itE} \langle \Phi(0)|\Phi(t)\rangle \, \mathrm{d}t, \qquad \text{(A14)}$$

where C is a normalization constant and Θ is the time up to which one has to integrate the TDSE in order to reach the desired energy resolution π/Θ. The Nyquist sampling theorem gives an upper bound to the time step that can be used. For the systems considered in the present paper, this bound is sufficiently small to guarantee that the errors in the eigenvalues are small (see Ref. [28] for a derivation of bounds, etc.).

Similarly, we can obtain the local DOS (LDOS) of the system for a particular pure state $|\Psi\rangle$, such as the initial state or final state of the system, by the formula

$$P(E) = \sum_n d_n^2 \delta(E - E_n) = \sum_n |\langle E_n|\Psi\rangle|^2 \delta(E - E_n)$$

$$= \frac{1}{2\pi} \int_{-\infty}^{+\infty} e^{itE} \langle \Psi| e^{-itH} |\Psi\rangle \, \mathrm{d}t$$

$$\approx C \int_{-\Theta}^{+\Theta} e^{itE} \langle \Psi| e^{-itH} |\Psi\rangle \, \mathrm{d}t, \qquad \text{(A15)}$$

where $|E_n\rangle$ are energy eigenstates and $d_n = \langle E_n|\Psi\rangle$. Note that the concept of typicality is not involved in the calculation of $P(E)$.

4. Simulation details

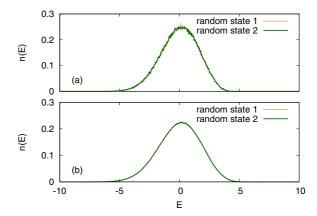The algorithm to compute the DOS $n(E)$ consists of the following steps:

FIG. 5. Simulation results for the density of states $n(E)$ for a quantum ladder system with (a) 18 spins and (b) 22 spins. Two random states are used to compute $n(E)$ according to the algorithm described in the text. The system Hamiltonian is defined by Eq. (7).

(1) Generate a random state $|\Phi(0)\rangle$ at $t = 0$.

(2) Copy this state to $|\Phi(t)\rangle$.

(3) Calculate $\langle \Phi(0)|\Phi(t)\rangle$ and store the result.

(4) Solve the TDSE for a small time step δt, replacing $|\Phi(t)\rangle$ with $|\Phi(t + \delta t)\rangle$.

(5) Repeat steps 3 and 4 K times.

(6) Compute the Fourier transform of the tabulated result.

In the simulation, we use $\delta t = 0.02$ for the second-order product-formula algorithm and repeat $K = 4096 \times 5$ steps. The total simulation time is $\Theta = 409.6$. Hence, the energy resolution is about $\pi/\Theta \approx 0.0077$. In principle, $n(E)$ may be averaged over different random states. It turns out that this is necessary only for small system sizes, as the error scales with the square root of the dimension of the Hilbert space. Figure 5 shows the simulation results for $n(E)$ obtained from two random states for systems with 18 and 22 spins. It can be clearly seen that the curves $n(E)$ obtained for two random states coincide apart from some small fluctuations. These fluctuations disappear for larger system sizes.

The procedure for numerically testing the Jarzynski relation is as follows:

(1) Generate the initial state $|\Psi(a, E_{\mathrm{ini}}, t = 0)\rangle$ by the Chebyshev-polynomial algorithm.

(2) Calculate the LDOS $P_{\mathrm{ini}}(E)$ for the initial state $|\Psi(a, E_{\mathrm{ini}}, t = 0)\rangle$.

(3) Solve the TDSE for the time-dependent Hamiltonian $H + h(t)$.

(4) Calculate the LDOS $P_{\mathrm{fin}}(E)$ for the final state $|\Psi(a, E_{\mathrm{ini}}, t = 2\tau)\rangle$.

(5) Repeat from step 3 for different process rates $\gamma = 1/2\tau$.

In the simulation, the parameters for the initial states are $a = 1000$ and $E_{\mathrm{ini}} = 0.42(L - 1)$, $L = N/2$, where N ranges from 18 to 30. We use $\delta t = 0.02$ for the second-order product-formula algorithm to solve the TDSE. After the whole process, we collect the data sets of $n(E)$, $\langle E \rangle_{\mathrm{ini}}$, $P_{\mathrm{ini}}(E)$, $\langle E \rangle_{\mathrm{fin}}$, and $P_{\mathrm{fin}}(E)$ for further analysis.

APPENDIX B: DATA AND ERROR ANALYSIS

Our goal is to test the validity of the Jarzynski relation beyond the Gibbsian initial state in isolated systems, i.e.,

$$\langle e^{-\beta W} \rangle = \int P_{\mathrm{W}}(W) \, e^{-\beta W} \, \mathrm{d}W = e^{-\beta \Delta F}, \qquad \text{(B1)}$$

where the work W is defined as $W = E_{\mathrm{fin}} - E_{\mathrm{ini}}$ according to the two-measurement scheme, $P_{\mathrm{W}}(W)$ is the work probability, and ΔF is the difference between the free energies of the two equilibrium states of the initial and final Hamiltonians. In principle, we must calculate both sides of Eq. (B1). The right-hand side (r.h.s.) equals 1, as the protocol we use [see Eq. (8)] ends with the same Hamiltonian as the initial one, and hence $\Delta F = 0$. Therefore, we only need to calculate the l.h.s., which requires information on the inverse temperature β and the work probability $P_W(W)$.

1. Estimation of the inverse temperature

The initial state is narrowly centered at the initial energy E_{ini} [as the standard deviation of $P_{\mathrm{ini}}(E)$ is about 0.03 for $a = 1000$]. A microcanonical temperature can be calculated according to the standard formula

$$\beta = \frac{\mathrm{d}}{\mathrm{d}E} \ln n(E); \qquad \text{(B2)}$$

cf. Eq. (6).

We get β from fitting $n(E)$ in the interval $[E_{\mathrm{ini}} - \epsilon, E_{\mathrm{ini}} + \epsilon]$, where E_{ini} is the initial mean energy and ϵ is a parameter to determine the range for fitting. The inverse temperature β does not vary significantly for $\epsilon \lesssim 0.5$ (see below).

2. Estimation of the work-probability function

As mentioned in the text, we have two nontrivial distributions of energy, a final and an initial one, from which P_W must be inferred. Without further assumptions, the attribution of a final and an initial distribution of energy to one distribution of work cannot be entirely unique. Thus, we rely on a further assumption: The probability distribution of work as arising from an initial δ distribution with regard to energy could in principle vary strongly with the position E_{ini} at which this initial distribution is peaked. Assuming that this is not the case in the small regime where $P_{\mathrm{ini}}(E)$ takes on non-negligible values, the probability distributions of work and energy are related as

$$P_{\mathrm{fin}}(E_{\mathrm{fin}}) = \int P_{\mathrm{ini}}(E_{\mathrm{ini}}) \, P_W(E_{\mathrm{fin}} - E_{\mathrm{ini}}) \, \mathrm{d}E_{\mathrm{ini}}. \qquad \text{(B3)}$$

Multiplying this equation by $e^{-\beta E_{\mathrm{fin}}}$ and integrating over E_{fin}, followed by a change of variables $E_{\mathrm{fin}} \to W + E_{\mathrm{ini}}$ on the r.h.s., yields

$$\frac{\int P_{\mathrm{fin}}(E_{\mathrm{fin}}) \, e^{-\beta E_{\mathrm{fin}}} \, \mathrm{d}E_{\mathrm{fin}}}{\int P_{\mathrm{ini}}(E_{\mathrm{ini}}) \, e^{-\beta E_{\mathrm{ini}}} \, \mathrm{d}E_{\mathrm{ini}}} = \int P_W(W) \, e^{-\beta W} \, \mathrm{d}W = \langle e^{-\beta W} \rangle \qquad \text{(B4)}$$

Thus, the l.h.s. of Eq. (B4) yields $\langle e^{-\beta W} \rangle$ based on P_{fin}, P_{ini} for different sweep rates γ.
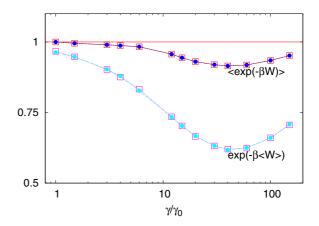

FIG. 6. Simulation results for $\langle e^{-\beta W} \rangle$ and $e^{-\beta \langle W \rangle}$ as a function of the process rate γ (normalized to the slowest rate, $\gamma_0 = 2.6 \times 10^{-4}$) for two random states $|\Phi\rangle$ (represented by squares and circles) used to prepare the initial state [see Eq. (A6)]. The system is a quantum ladder with 22 spins. The initial energy corresponds to the inverse temperature $\beta = 1.23$ (see Fig. 2, inset).

3. Estimation of work averages

In order to calculate the l.h.s. of Eq. (B1), i.e., $\langle e^{-\beta W} \rangle$, we do not have to really calculate the work probability. As explained before, we can use Eq. (B4). Similarly, we have

$$\langle W \rangle = \int P_{\mathrm{fin}}(E_{\mathrm{fin}}) \, E_{\mathrm{fin}} \, \mathrm{d}E_{\mathrm{fin}} - \int P_{\mathrm{ini}}(E_{\mathrm{ini}}) \, E_{\mathrm{ini}} \, \mathrm{d}E_{\mathrm{ini}}$$
$$= \langle E_{\mathrm{fin}} \rangle - \langle E_{\mathrm{ini}} \rangle \qquad \text{(B5)}$$

and

$$e^{-\beta \langle W \rangle} = e^{-\beta(\langle E_{\mathrm{fin}} \rangle - \langle E_{\mathrm{ini}} \rangle)}. \qquad \text{(B6)}$$

Hence, the calculations of $\langle e^{-\beta W} \rangle$ and $e^{-\beta \langle W \rangle}$ solely depend on the data set obtained from the simulation.

Figure 6 presents the simulation results for $\langle e^{-\beta W} \rangle$ and $e^{-\beta \langle W \rangle}$ as a function of the process rate of the magnetic field imposed on the two legs of the ladder for 22 spins. The inverse temperature β is set to 1.23 (see Fig. 2). Two random states are used to prepare the initial state of the system. It can be seen that $\langle e^{-\beta W} \rangle$ and $e^{-\beta \langle W \rangle}$ calculated for these two initial states do not differ much. Hence, it is sufficient to study the JR for only one particular initial state.

4. Size of errors

The main error of our overall analysis is set neither by our numerical methods (finite time step, maximum time) nor by the specific realization of the initial state. Instead, the main error results when determining the inverse temperature β by fitting the DOS locally. By varying the fit range $[E_{\mathrm{ini}} - \epsilon, E_{\mathrm{ini}} + \epsilon]$ from $\epsilon = 0.25$ to $\epsilon = 0.5$, we find that the value of β can be determined with a precision of $\approx 5\%$ [see the small error bars in Fig. 4(c)]. This precision implies that, for the sweep rate $\gamma/\gamma_0 = 40$, the quantity $\langle e^{-\beta W} \rangle$ has a corresponding error of $\approx 2\%$. This error is comparable with the symbol size used and not indicated explicitly in Fig. 4(a). We can therefore exclude that the deviation of this quantity from 1 for such values of γ is an artifact of our approach.

However, the corresponding error for the shift δE is much larger since

$$\delta E = -\frac{1}{\beta} \ln\langle e^{-\beta W}\rangle \qquad (B7)$$

essentially is the logarithm of a small number <1. Consequently, the corresponding error can be as large as $\approx 30\%$ [see the error bars in Fig. 4(c)]. Such errors in δE are particularly relevant for the quality of the finite-size scaling $\delta E(L)$ and thus taken into account in the conclusions.

5. Finite-size scaling

A central result of this paper concerns the upscaling of the system towards the limit $L \to \infty$. It is instructive to make comparisons with a set of M disconnected small systems: The work-probability distribution in this case is an M-fold convolution of the work-probability distribution as resulting for each small system. Since mean values are additive under convolution, one gets the corresponding shift scaling as $\delta E(M) = M\delta E(1)$. The standard deviation of the work-probability distribution, however, scales under convolution as $\Delta E(M) = \sqrt{M}\Delta E(1)$. This implies that, for large M, $\delta E(M)$ becomes inevitably larger than $\Delta E(M)$ and thus the resulting work-probability distribution is far away from fulfilling the JR. Therefore, in the limit of many disconnected small systems, the JR is strongly violated whenever $\delta E(1)$ is nonzero. This finding is clearly different from a long connected ladder, as discussed in the paper.

[1] S. Popescu, A. J. Short, and A. Winter, Nature Phys. **2**, 754 (2006).

[2] S. Goldstein, J. L. Lebowitz, R. Tumulka, and N. Zanghì, Phys. Rev. Lett. **96**, 050403 (2006).

[3] P. Reimann, Phys. Rev. Lett. **101**, 190403 (2008).

[4] P. Reimann, Phys. Rev. Lett. **115**, 010403 (2015).

[5] J. Eisert, M. Friesdorf, and C. Gogolin, Nature Phys. **11**, 124 (2015).

[6] C. Gogolin and J. Eisert, Rep. Prog. Phys. **79**, 056001 (2016).

[7] M. Rigol, V. Dunjko, and M. Olshanii, Nature **452**, 854 (2008).

[8] R. Steinigeweg, J. Herbrych, and P. Prelovšek, Phys. Rev. E **87**, 012118 (2013).

[9] W. Beugeling, R. Moessner, and M. Haque, Phys. Rev. E **89**, 042112 (2014).

[10] R. Steinigeweg, A. Khodja, H. Niemeyer, C. Gogolin, and J. Gemmer, Phys. Rev. Lett. **112**, 130403 (2014).

[11] A. S. L. Malabarba, L. P. García-Pintos, N. Linden, T. C. Farrelly, and A. J. Short, Phys. Rev. E **90**, 012121 (2014).

[12] P. Reimann, Nat. Commun. **7**, 10821 (2016).

[13] H. Niemeyer, K. Michielsen, H. De Raedt, and J. Gemmer, Phys. Rev. E **89**, 012131 (2014).

[14] J. Gemmer and R. Steinigeweg, Phys. Rev. E **89**, 042113 (2014).

[15] D. Schmidtke and J. Gemmer, Phys. Rev. E **93**, 012125 (2016).

[16] U. Seifert, Eur. Phys. J. B **64**, 423 (2008).

[17] M. Esposito, U. Harbola, and S. Mukamel, Rev. Mod. Phys. **81**, 1665 (2009).

[18] C. Jarzynski, Annu. Rev. Condens. Matter Phys. **2**, 329 (2011).

[19] A. J. Roncaglia, F. Cerisola, and J. P. Paz, Phys. Rev. Lett. **113**, 250601 (2014).

[20] P. Hänggi and P. Talkner, Nature Phys. **11**, 108 (2015).

[21] P. Talkner, P. Hänggi, and M. Morillo, Phys. Rev. E **77**, 051131 (2008).

[22] M. Campisi, Phys. Rev. E **78**, 012102 (2008).

[23] P. Talkner, M. Morillo, J. Yi, and P. Hänggi, New J. Phys. **15**, 095001 (2013).

[24] M. Campisi, P. Hänggi, and P. Talkner, Rev. Mod. Phys. **83**, 771 (2011).

[25] Here, we assume that the spectrum is nondegenerate.

[26] M. Srednicki, Phys. Rev. E **50**, 888 (1994).

[27] J. M. Deutsch, Phys. Rev. A **43**, 2046 (1991).

[28] A. Hams and H. De Raedt, Phys. Rev. E **62**, 4365 (2000).

[29] R. Steinigeweg, J. Gemmer, and W. Brenig, Phys. Rev. Lett. **112**, 120601 (2014).

[30] R. Steinigeweg, J. Herbrych, X. Zotos, and W. Brenig, Phys. Rev. Lett. **116**, 017202 (2016).

[31] N. Y. Halpern and C. Jarzynski, Phys. Rev. E **93**, 052144 (2016).

[32] C. Jarzynski, Phys. Rev. E **73**, 046105 (2006).

[33] M. Stephan and J. Docter, J. Large-Scale Res. Facil. **1**, A1 (2015).

[34] H. De Raedt, Comput. Phys. Rep. **7**, 1 (1987).

[35] H. De Raedt and K. Michielsen, in *Handbook of Theoretical and Computational Nanotechnology*, edited by M. Rieth and W. Schommers (American Scientific, Los Angeles, 2006), pp. 2–48.

[36] H. Tal-Ezer and R. Kosloff, J. Chem. Phys. **81**, 3967 (1984).

[37] V. V. Dobrovitski and H. A. De Raedt, Phys. Rev. E **67**, 056702 (2003).

[38] V. A. Ngo and S. Haas, arXiv:1303.2141.